Electronic Supplementary Material (ESI) for Physical Chemistry Chemical Physics.

Computational Assessment of the Crystallization Tendency of 1-Ethyl-3-methylimidazolium Ionic Liquids

Supporting Information

Ctirad Červinka[*]*, Vojtěch Štejfa*

[†] Department of Physical Chemistry, University of Chemistry and Technology Prague, Technická 5, CZ-166 28 Prague 6, Czech Republic

*Corresponding author: cervinkc@vscht.cz

TABLE S1

Atomic charges parametrized in this work for the [HSO_4] anion, using the CHELPG procedure and the B3LYP/aug-cc-pVTZ levels of theory.

Atom type	Charge, q_e
SO	1.389
OS	-0.696
OH	-0.649
HO	0.348

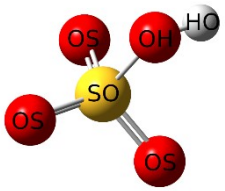

TABLE S2

Overview of 1-ethyl-3-methylimidazolium ionic liquids included in this study along with their experimental unit-cell parameters *a*, *b*, *c*, and *β* and number of ion pairs forming the unit cell *Z*.

Ionic liquid	CAS RN	CSD refcode	Space group	*Z*	*a*, Å	*b*, Å	*c*, Å	*β*, deg.
[emIm][Br]	65039-08-9	ZIBHUN01[1]	$P2_1/c$	4	8.674	7.881	12.436	109.26
[emIm][BF_4]	143314-16-3	LAZRIO01[2]	$P2_1/c$	4	8.653	9.285	13.217	121.36
[emIm][PF_6]	155371-19-0	HAYBUE02[3]	$P2_1/c$	4	8.627	9.035	13.469	101.92
[emIm][NO_3]	143314–14-1	KUCPED[4]	$P2_1/n$	4	4.540	14.810	13.445	95.74
[emIm][SCN]	331717–63-6							
[emIm][DCA]	370865-89-7							
[emIm][TCM]	666823–18-3							
[emIm][$MeSO_3$]	145022-45-3	SAGPOJ[5]	$P2_1/a$	4	12.020	14.978	5.583	95.75
[emIm][HSO_4]	412009-61-1	WAKDAR[6]	$Pb2_1a$	4	15.918	7.923	7.419	90.00
[emIm][$MeSO_4$]	516474–01-4							
[emIm][$EtSO_4$]	342573-75-5							
[emIm][AcO]	143314–17-4							
[emIm][TFA]	174899-65-1							
[emIm][OTf]	145022–44-2	RENSIN[7]	Pbca	8	10.183	12.384	18.294	90.00
[emIm][TFES]	880084-63-9	POYLIZ[8]	$P2_1/n$	4	8.770	9.766	14.282	95.36
[emIm][OTs]	328090–25-1	UYUJUV02[9]	$P2_1/c$	8	8.958	30.874	10.112	90.94
[emIm][Me_2PO_4]	945611–27-8	COVLAD[10]	P-1	2	7.632	8.640	10.028	100.43[a]
[emIm][Et_2PO_4]	848641-69-0							
[emIm][Bu_2PO_4]	869858-84-4							
[emIm][NTf_2]	174899-82-2	RENSEJ01[11]	$Pna2_1$	8	27.713	7.0343	15.769	90.00

[a] α=91.62°, γ=111.94°.

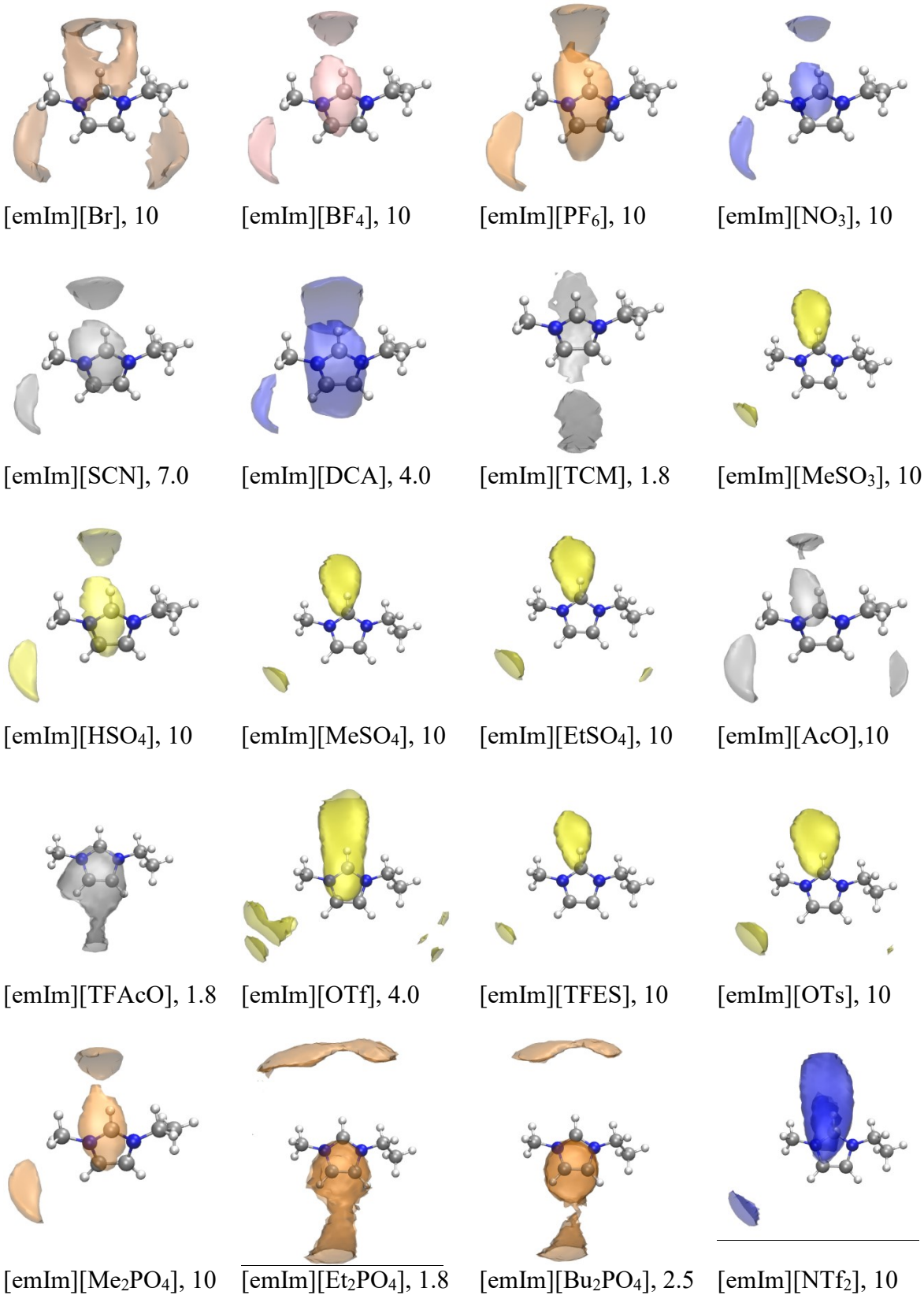

FIGURE S1. Contours of the spatial distribution functions (SDF) of anionic central atoms around the [emIm] cation, corresponding to the given SDF values.

TABLE S3

Overview of the calculated structural parameters used for data interpretations and correlations. The following parameters are given: position of the first peak of the cation-anion radial distribution function d_{int}, intensity of the first RDF peak g_{RDF}^{max}, integral coordination numbers n_{coord}^{CR} and n_{coord}^{CW} of cation-anion CR-X and CW-X contacts, molar volume at 400 K, isobaric thermal expansivity coefficient α_p, and cohesive energy density E_ρ.

Ionic liquid	d_{int}, Å	g_{RDF}^{max}	n_{coord}^{CR}	n_{coord}^{CW}	V_m, cm^3 mol^{-1}	α_p, MK^{-1}	$-E_\rho$, kJ cm^{-3}
[emIm][Br]	3.60	3.23	1.63	1.40	137.9	430.2	1.40
[emIm][BF_4]	3.29	1.77	3.90	3.02	166.8	510.8	1.00
[emIm][PF_6]	3.34	1.56	4.96	1.17	188.4	510.9	0.92
[emIm][NO_3]	3.22	2.06	3.33	2.60	143.9	416.5	1.25
[emIm][SCN]	3.37	2.25	1.36	1.11	156.2	453.9	1.11
[emIm][DCA]	3.53	1.45	1.36	2.14	170.1	517.4	0.93
[emIm][TCM]	3.39	2.09	3.08	3.40	198.0	580.2	0.78
[emIm][$MeSO_3$]	3.34	2.18	3.08	2.38	179.0	436.3	0.93
[emIm][HSO_4]	3.40	1.5	0.88	0.69	162.8	446.9	1.20
[emIm][$MeSO_4$]	3.35	2.15	3.12	2.32	184.3	421.2	1.00
[emIm][$EtSO_4$]	3.35	1.87	2.44	2.25	202.0	424.6	0.93
[emIm][AcO]	3.26	2.46	2.13	1.56	160.8	424.4	1.08
[emIm][TFA]	3.27	2.51	2.07	1.22	178.9	497.5	0.92
[emIm][OTf]	3.41	3.04	3.13	2.48	198.7	450.5	0.82
[emIm][TFES]	3.28	2.25	2.71	2.09	215.5	507.6	0.77
[emIm][OTs]	3.35	2.74	2.87	2.12	247.2	415.5	0.76
[emIm][Me_2PO_4]	3.32	2.64	2.00	1.42	209.0	481.9	0.80
[emIm][Et_2PO_4]	3.32	3.21	1.99	1.41	245.0	503.2	0.73
[emIm][Bu_2PO_4]	3.31	4.34	1.93	1.42	320.6	565.4	0.59
[emIm][NTf_2]	3.32	2.03	3.01	2.83	260.6	523.9	0.62

TABLE S4

Overview of the original experimental studies used in this work to derive the reference experimental density and isobaric thermal expansivity, both at the standard pressure.

Reference	Data points	Temperature range, K
[emIm][BF_4]		
Seki et al.[12]	15	283-353
Song et al.[14]	11	293-343
Navia et al.[16]	9	298-308
Watanabe et al.[18]	9	293-363
Montalbán et al.[20]	6	293.343
Currás et al.[22]	5	293-333
Bhagour et al.[24]	4	293-308
Gupta et al.[26]	4	293-308
Rao et al.[28]	4	293-323
Sharma[30]	4	293-308
[emIm][$MeSO_4$]		
Costa et al.[32]	71	293-363
Tomé et al.[34]	8	293-393
Ficke et al.[36]	7	293-343
Tsamba et al.[37]	5	298-342
Alkhaldi et al.[38]	4	298-313
Sandhya et al.[40]	3	298-308
-	-	-

Reference	Data points	Temperature range, K
[emIm][NTf_2]		
Součková et al.[13]	21	261-363
Fröba et al.[15]	19	273-363
Rocha et al.[17]	17	278-358
Zorębski et al.[19]	17	293-363
Seoane et al.[21]	11	293-343
Khalil et al.[23]	9	293-333
Dzida et al.[25]	8	278-363
Safarov et al.[27]	7	283-363
Song et al.[29]	7	283-333
Yao et al.[31]	7	293-323
Montalbán et al.[20]	7	293-343
Tokuda et al.[33]	7	288-313
Anwar et al.[35]	6	298-323
Tokuda et al.[33]	7	288-313
Anwar et al.[35]	6	298-323
Batista et al.[39]	4	298-328
Salinas et al.[41]	4	278-338
Vuksanovic et al.[42]	4	288-318

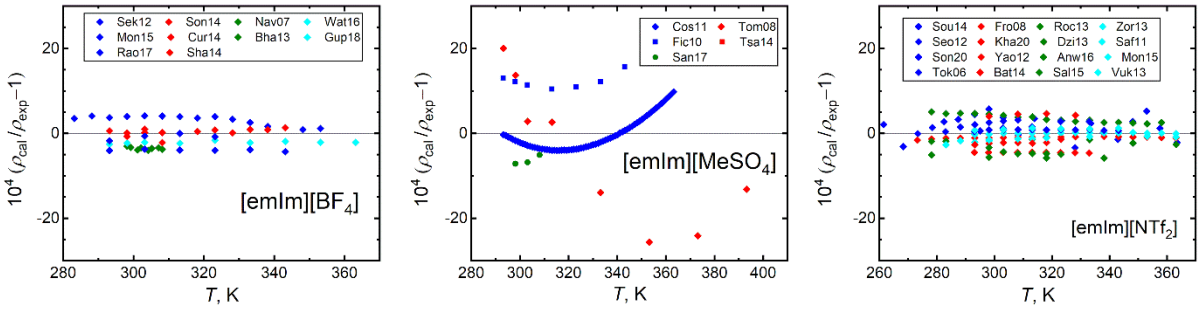

FIGURE S2. Deviation plots for selected experimental data sets on liquid phase densities for three ILs, exhibiting mutual consistency with the uncertainties stated with the authors (0.15 % on average)

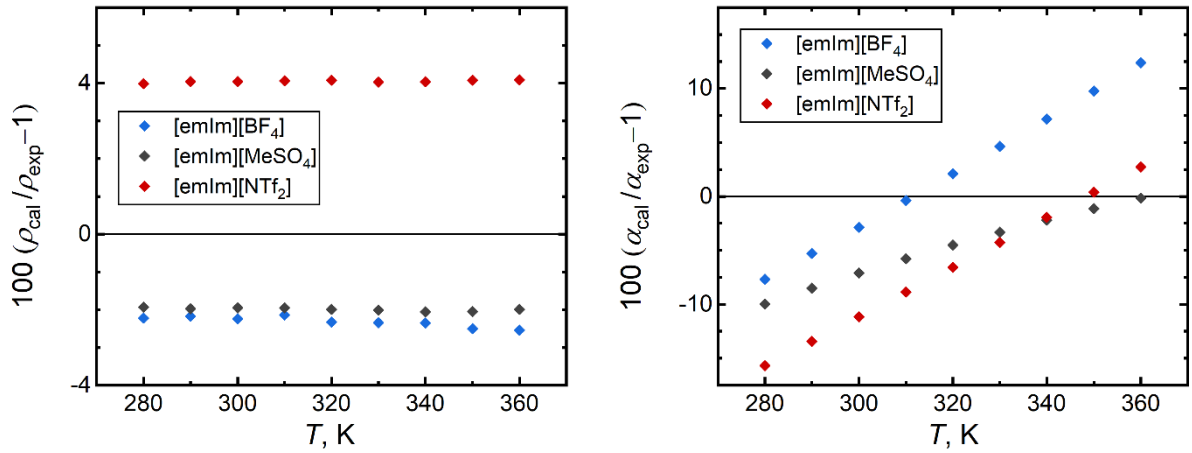

FIGURE S3. Relative deviations of densities ρ and isobaric thermal expansivities α calculated from the MD simulations using the CL&P force field from the averaged experimental data.

TABLE S5

Overview of the calculated energetic parameters used for data interpretations and correlations. The following parameters are given: pair interaction energy $E_{\mathrm{int}}^{\mathrm{liq}}$ calculated for the closest ion pairs in their average mutual geometry in the liquid phase, pair interaction energy $E_{\mathrm{int}}^{\mathrm{gas}}$ calculated for an isolated ion pair at the sSAPT0/jun-pVDZ and MP2C-F12/aug-cc-pVDZ levels of theory, Conformational penalty $\Delta E_{\mathrm{conf}}^{\mathrm{cond}}$ associated with condensation, change of the total energy upon vaporization $\Delta_{\mathrm{vap}}U$, relative increase of the contribution of dispersion interactions $\varepsilon_{\mathrm{disp}}$ for the cohesion between liquid and gas phase, curvature κ of the ion pair interaction energy – distance curve at its minimum.

Ionic liquid	$-E_{\mathrm{int}}^{\mathrm{liq}}$, kJ mol^{-1}	$-E_{\mathrm{int,SAPT}}^{\mathrm{gas}}$, kJ mol^{-1}	$-E_{\mathrm{int,MP2C}}^{\mathrm{gas}}$, kJ mol^{-1}	$\Delta E_{\mathrm{conf}}^{\mathrm{cond}}$, kJ mol^{-1}	$\Delta_{\mathrm{vap}}U$, kJ mol^{-1}	$\frac{\varepsilon_{\mathrm{disp}}^{\mathrm{liq}}}{\varepsilon_{\mathrm{disp}}^{\mathrm{gas}}}$	$\varepsilon_{\mathrm{disp}}^{\mathrm{liq}}$	κ, kJ mol^{-1}Å^{-2}
[emIm][Br]	346.0	369.6	322.2	23.6	193.7	3.83	0.25	296
[emIm][BF4]	331.3	371.5	375.0	40.1	167.4	5.45	0.30	355
[emIm][PF6]	313.3	347.3	352.4	34.0	173.4	5.02	0.32	313
[emIm][NO3]	357.2	384.4	389.2	27.2	180.1	5.01	0.37	389
[emIm][SCN]	336.5	373.0	379.6	36.5	173.2	3.64	0.33	284
[emIm][DCA]	325.8	358.7	367.5	32.9	157.6	3.57	0.38	215
[emIm][TCM]	271.5	345.1	351.0	73.7	154.2	4.16	0.37	190
[emIm][MeSO3]	365.0	413.5	411.1	48.5	166.9	5.20	0.43	425
[emIm][HSO4]	350.0	387.8	394.0	37.8	195.4	4.75	0.38	368
[emIm][MeSO4]	392.5	394.5	396.2	42.5	183.7	4.77	0.42	337
[emIm][EtSO4]	352.2	395.1	398.3	42.9	187.6	5.66	0.44	354
[emIm][AcO]	408.1	450.7	437.6	42.6	173.5	5.88	0.40	476
[emIm][TFA]	349.8	392.2	389.0	42.4	163.9	4.74	0.40	314
[emIm][OTf]	330.5	364.2	370.6	33.8	162.6	5.12	0.43	344
[emIm][TFES]	324.0	362.2	367.0	38.2	165.2	4.15	0.43	298
[emIm][OTs]	357.0	407.9	402.2	50.9	187.4	4.85	0.52	419
[emIm][Me2PO4]	382.0	429.4	422.9	47.4	168.2	5.32	0.43	459
[emIm][Et2PO4]	351.4	432.4	424.4	81.1	177.9	5.03	0.45	494
[emIm][Bu2PO4]	358.4	432.3	425.9	73.9	188.8	3.93	0.50	382
[emIm][NTf2]	316.3	355.7	358.4	39.4	162.2	4.97	0.53	333

TABLE S6

Overview of the calculated diffusion parameters used for data interpretations and correlations. The following parameters are given: cationic self-diffusivity D_{cat}, anionic self-diffusivity D_{ani}, activation energy for the diffusion of the ion pair E_A^{dif}, all at 400 K.

Ionic liquid	$-\log(D_{cat})$	$-\log(D_{ani})$	E_A^{dif}, kJ mol^{-1}
[emIm][Br]	10.76	10.96	43.40
[emIm][BF_4]	9.87	10.12	24.61
[emIm][PF_6]	10.26	10.54	34.06
[emIm][NO_3]	10.22	10.37	26.18
[emIm][SCN]	9.88	9.94	29.06
[emIm][DCA]	9.63	9.58	17.68
[emIm][TCM]	9.59	9.56	17.70
[emIm][$MeSO_3$]	10.14	10.40	32.73
[emIm][HSO_4]	10.36	10.44	39.93
[emIm][$MeSO_4$]	10.09	10.39	26.85
[emIm][$EtSO_4$]	10.20	10.55	29.56
[emIm][AcO]	10.09	10.31	27.37
[emIm][TFA]	9.95	10.15	26.89
[emIm][OTf]	10.10	10.42	29.47
[emIm][TFES]	10.06	10.24	25.25
[emIm][OTs]	10.47	10.81	38.40
[emIm][Me_2PO_4]	9.83	10.18	22.97
[emIm][Et_2PO_4]	10.15	10.53	28.33
[emIm][Bu_2PO_4]	10.54	10.79	41.24
[emIm][NTf_2]	9.99	10.19	24.11

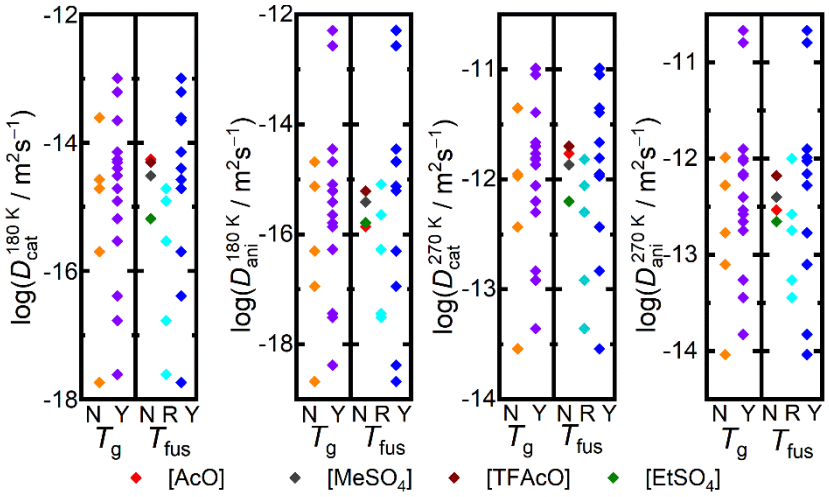

FIGURE S4. Comparison of cationic and anionic self-diffusivities (D_{cat}, D_{ani}) of for groups of ionic liquids at 180 K and 270 K sorted upon availability of T_g (Yes in purple, No in orange) and T_{fus} (Yes in blue, Rarely crystallizing in cyan, No marked individually). Left – cationic self-diffusivity D_{cat}; center – anionic self-diffusivity D_{ani}; right – activation energy for the diffusion of the ion pair E_A^{dif}.

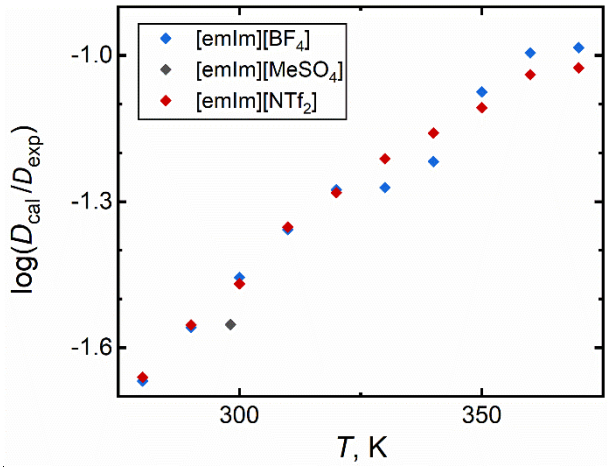

FIGURE S5. Logarithmic errors of self-diffusivities of the ion pair D calculated from the MD simulations using the CL&P force field from the experimental data.

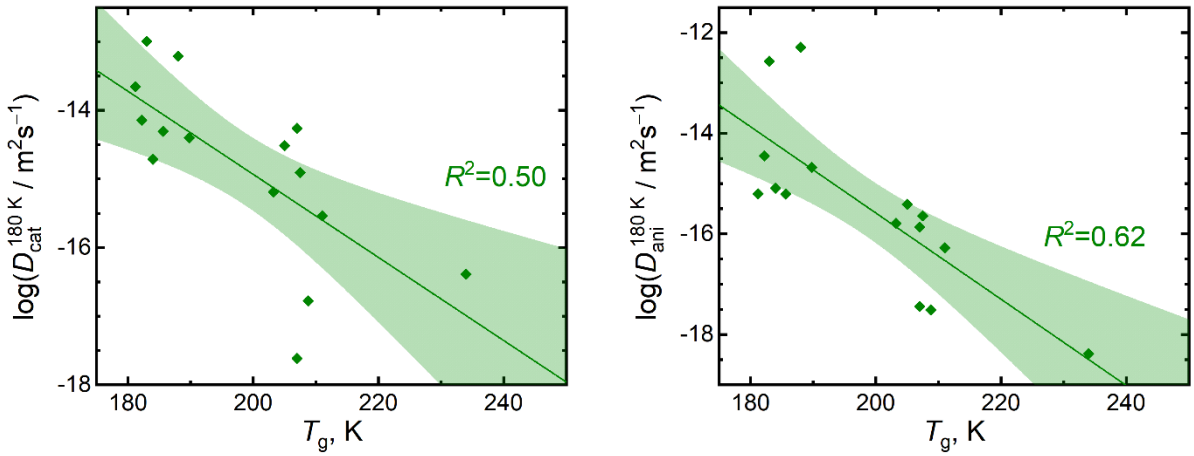

FIGURE S6. Correlations of the experimental glass transition temperatures T_g with the calculated cationic and anionic self-diffusivities D_{cat} and D_{ani} extrapolated to 180 K, respectively, along with the 95% confidence intervals for the correlation.

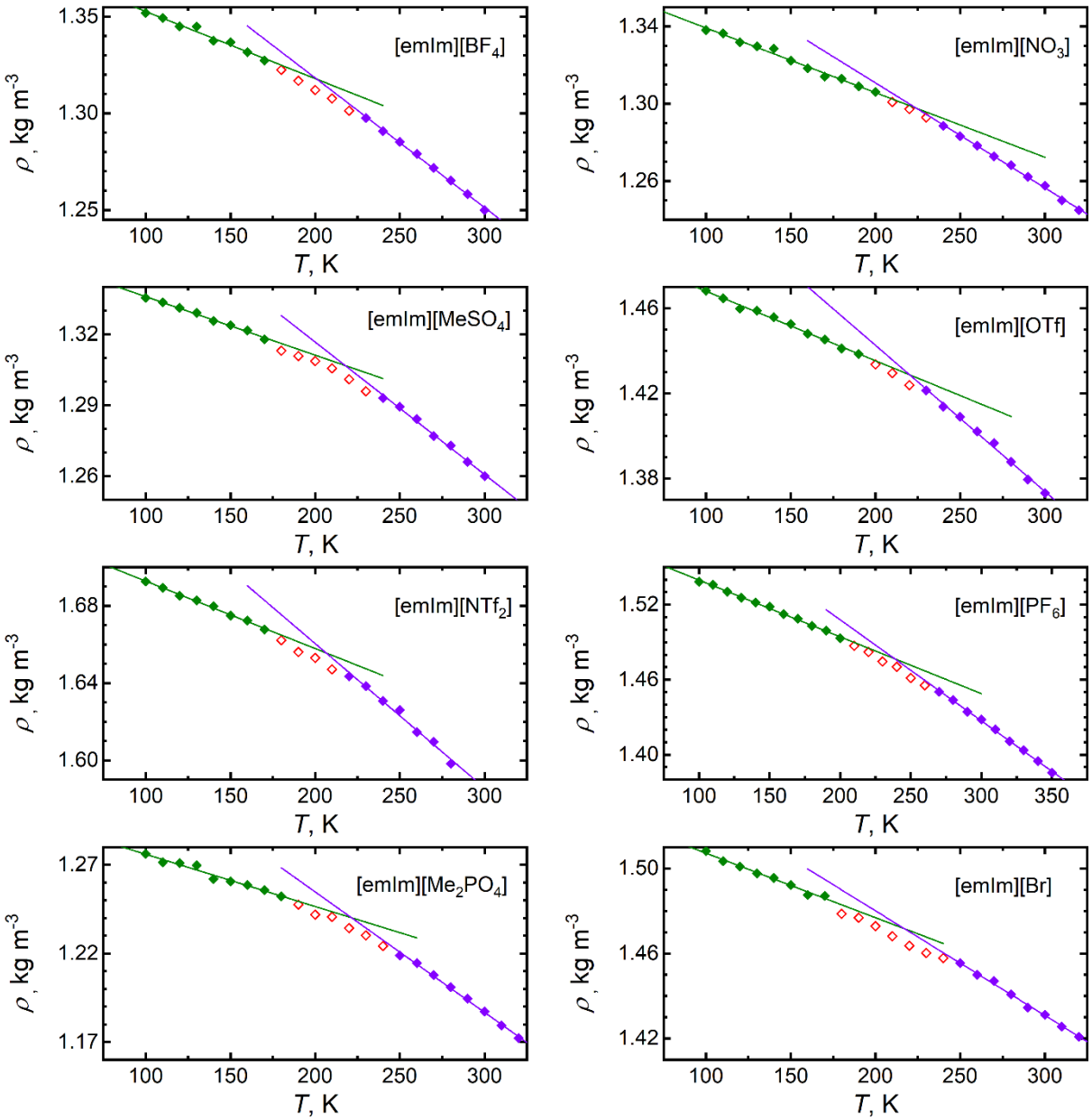

FIGURE S7. Illustration of the procedure followed to calculate the T_g from the temperature-dependent densities obtained from the MD simulations using the CL&P force field. Green and purple points used for extrapolations of the trends of the glassy and liquid phases, respectively. Empty red points were excluded from evaluation of T_g.

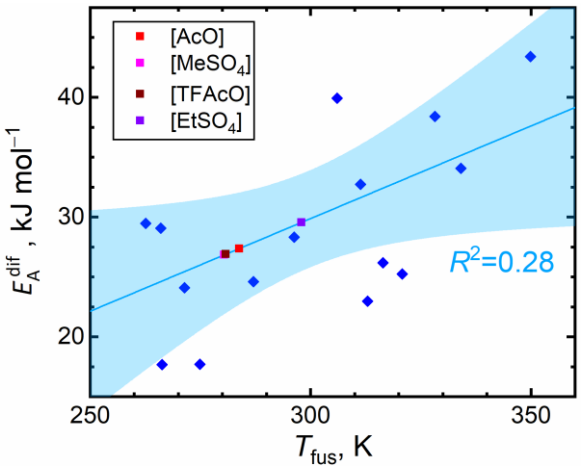

FIGURE S8. Correlation of the experimental melting temperatures T_{fus} with the activation energy for the diffusion of an ion pair calculated at 400 K along with the 95% confidence intervals for the correlation.

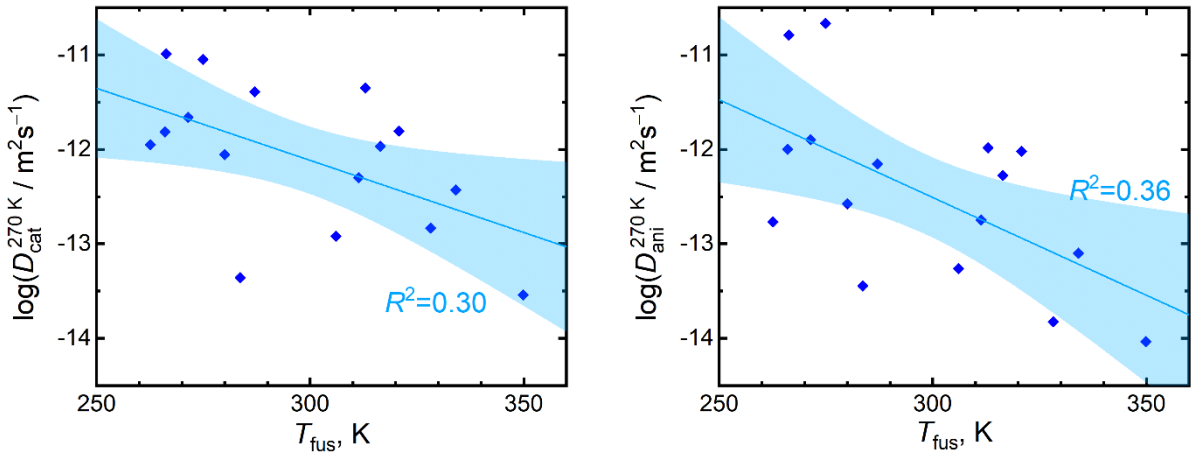

FIGURE S9. Correlations of the experimental melting temperatures T_{fus} with the calculated cationic and anionic self-diffusivities D_{cat} and D_{ani} extrapolated to 270 K, respectively, along with the 95% confidence intervals for the correlation.

TABLE S7
Overview of the Pearson correlation coefficients R of various correlations of T_g or T_{fus} with properties obtained from molecular dynamics or quantum chemical calculations. The most significant correlations are highlighted with R values given in bold.

Correlation	T_g	T_{fus}	Correlation	T_g	T_{fus}	Correlation	T_g	T_{fus}
E_{int}^{liq}	−0.56	−0.36	κ	**+0.67**	+0.31	α_p	−0.56	−0.45
E_{int}^{gas}	**−0.68**	−0.17	d_{int}	−0.09	+0.02	E_ρ	+0.05	−0.39
ΔE_{conf}^{cond}	+0.18	−0.24	g_{RDF}^{max}	+0.38	+0.04	$\log(D_{cat})$	**−0.79**	**−0.64**
$\Delta_{vap}U$	**+0.71**	**+0.56**	n_{coord}	−0.04	+0.01	$\log(D_{ani})$	**−0.77**	**−0.64**
$\frac{\varepsilon_{disp}^{liq}}{\varepsilon_{disp}^{gas}}$	+0.33	+0.17	V_m	+0.29	−0.20	E_A^{dif}	**+0.72**	+0.53

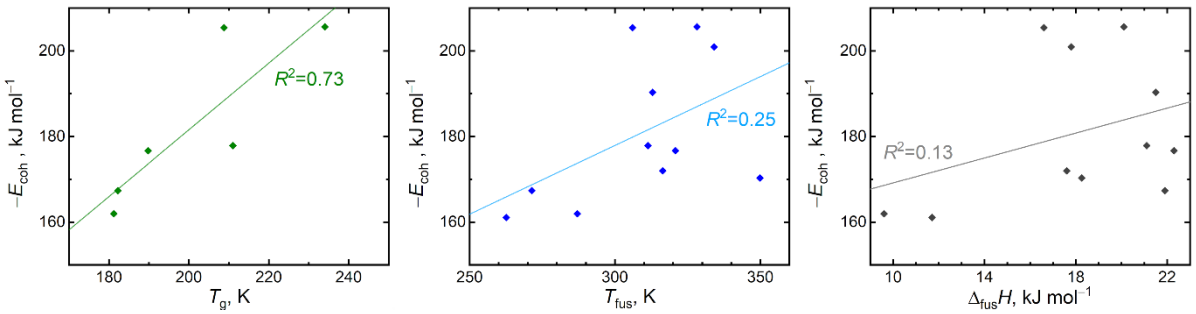

FIGURE S10. Correlation of the experimental glass transition temperature T_g, melting temperatures T_{fus}, and fusion enthalpy $\Delta_{fus}H$ with the PBE-D3/PAW cohesive energies of the 11 crystalline ionic liquids with available crystal structures.

TABLE S8
Overview of the Pearson correlation coefficients R of various correlations of $\Delta_{fus}H$ with properties obtained from molecular dynamics or quantum chemical calculations.

Correlation	$\Delta_{fus}H$	Correlation	$\Delta_{fus}H$	Correlation	$\Delta_{fus}H$
E_{int}^{liq}	−0.45	κ	+0.35	α_p	−0.02
E_{int}^{gas}	−0.49	d_{int}	−0.14	E_ρ	+0.31
ΔE_{conf}^{cond}	+0.12	g_{RDF}^{max}	+0.30	$\log(D_{cat})$	−0.33
$\Delta_{vap}U$	−0.25	n_{coord}	−0.33	$\log(D_{ani})$	−0.33
$\frac{\varepsilon_{disp}^{liq}}{\varepsilon_{disp}^{gas}}$	−0.18	V_m	+0.49	E_A^{dif}	+0.25

References for the SI

1. P. M. Dean, B. R. Clare, V. Armel, et al., *Aust. J. Chem.*, 2009, **62**, 334-340.
2. K. Matsumoto, R. Hagiwara, Z. Mazej, et al., *Solid State Sci.*, 2006, **8**, 1250-1257.
3. W. M. Reichert, J. D. Holbrey, R. P. Swatloski, et al., *Cryst. Growth Des.*, 2007, **7**, 1106-1114.
4. J. S. Wilkes and M. J. Zaworotko, *J. Chem. Soc., Chem. Commun.*, 1992, **13**, 965-967.
5. V. Štejfa, J. Rohlíček and C. Červinka, *J. Chem. Thermodyn.*, 2021, 10.1016/j.jct.2021.106392.
6. V. Štejfa, J. Rohlíček and C. Červinka, 2020, 10.5517/ccdc.csd.cc5526pnsc.
7. A. R. Choudhury, N. Winterton, A. Steiner, et al., *CrystEngComm*, 2006, **8**, 742-745.
8. M. A. Harmer, C. P. Junk, V. V. Rostovtsev, et al., *Green Chem.*, 2009, **11**, 517-525.
9. W. Beichel, U. P. Preiss, B. Benkmil, et al., *Z. Anorg. Allg. Chem.*, 2013, **639**, 2153-2161.
10. V. Štejfa, J. Rohlíček and C. Červinka, *J. Chem. Thermodyn.*, 2020, **142**, 106020.
11. Y. U. Paulechka, G. J. Kabo, A. V. Blokhin, et al., *J. Phys. Chem. B*, 2009, **113**, 9538-9546.
12. S. Seki, S. Tsuzuki, K. Hayamizu, et al., *J. Chem. Eng. Data*, 2012, **57**, 2211-2216.
13. M. Součková, J. Klomfar and J. Pátek, *J. Chem. Thermodyn.*, 2014, **77**, 31-39.
14. D. Song and J. Chen, *J. Chem. Eng. Data*, 2014, **59**, 257-262.
15. A. P. Fröba, H. Kremer and A. Leipertz, *J. Phys. Chem. B*, 2008, **112**, 12420-12430.
16. P. Navia, J. Troncoso and L. Romaní, *J. Chem. Eng. Data*, 2007, **52**, 1369-1374.
17. M. A. A. Rocha, C. M. S. S. Neves, M. G. Freire, et al., *J. Phys. Chem. B*, 2013, **117**, 10889-10897.
18. M. Watanabe, D. Kodama, T. Makino, et al., *Fluid Ph. Equilibr.*, 2016, **420**, 44-49.
19. E. Zorębski, M. Geppert-Rybczyńska and M. Zorębski, *J. Phys. Chem. B*, 2013, **117**, 3867-3876.
20. M. G. Montalbán, C. L. Bolívar, F. G. Díaz Baños, et al., *J. Chem. Eng. Data*, 2015, **60**, 1986-1996.
21. R. G. Seoane, S. Corderí, E. Gómez, et al., *Ind. Eng. Chem. Res.*, 2012, **51**, 2492-2504.
22. M. R. Currás, P. Husson, A. A. H. Pádua, et al., *Ind. Eng. Chem. Res.*, 2014, **53**, 10791-10802.
23. R. Khalil, N. Chaabene, M. Azar, et al., *Fluid Ph. Equilibr.*, 2020, **503**, 112316.
24. S. Bhagour, S. Solanki, N. Hooda, et al., *J. Chem. Thermodyn.*, 2013, **60**, 76-86.
25. M. Dzida, M. Chorążewski, M. Geppert-Rybczyńska, et al., *J. Chem. Eng. Data*, 2013, **58**, 1571-1576.
26. H. Gupta, S. Malik, M. Chandrasekhar, et al., *J. Therm. Anal. Calorim.*, 2018, **131**, 1653-1669.
27. J. Safarov, W. A. El-Awady, A. Shahverdiyev, et al., *J. Chem. Eng. Data*, 2011, **56**, 106-112.
28. V. S. Rao, T. V. Krishna, T. M. Mohan, et al., *J. Chem. Thermodyn.*, 2017, **104**, 150-161.
29. T. Song, M. J. Lubben and J. F. Brennecke, *Fluid Ph. Equilibr.*, 2020, **504**, 112334.
30. V. K. Sharma, S. Solanki and S. Bhagour, *J. Chem. Eng. Data*, 2014, **59**, 1140-1157.

31. H. Yao, S. Zhang, J. Wang, et al., *J. Chem. Eng. Data*, 2012, **57**, 875-881.
32. A. J. L. Costa, J. M. S. S. Esperança, I. M. Marrucho, et al., *J. Chem. Eng. Data*, 2011, **56**, 3433-3441.
33. H. Tokuda, S. Tsuzuki, M. A. B. H. Susan, et al., *J. Phys. Chem. B*, 2006, **110**, 19593-19600.
34. L. I. N. Tomé, P. J. Carvalho, M. G. Freire, et al., *J. Chem. Eng. Data*, 2008, **53**, 1914-1921.
35. N. Anwar, Riyazuddeen and S. Yasmeen, *J. Mol. Liq.*, 2016, **224**, 189-200.
36. L. E. Ficke, R. R. Novak and J. F. Brennecke, *J. Chem. Eng. Data*, 2010, **55**, 4946-4950.
37. B. E. M. Tsamba, S. Sarraute, M. Traïkia, et al., *J. Chem. Eng. Data*, 2014, **59**, 1747-1754.
38. K. H. A. E. Alkhaldi, A. S. Al-Jimaz and M. S. AlTuwaim, *J. Chem. Thermodyn.*, 2017, **110**, 175-185.
39. M. L. S. Batista, L. I. N. Tomé, C. M. S. S. Neves, et al., *J. Mol. Liq.*, 2014, **192**, 26-31.
40. M. S. Sandhya, V. Govinda, I. Bahadur, et al., *J. Mol. Liq.*, 2017, **240**, 613-621.
41. R. Salinas, J. Pla-Franco, E. Lladosa, et al., *J. Chem. Eng. Data*, 2015, **60**, 525-540.
42. J. M. Vuksanovic, M. S. Calado, G. R. Ivanis, et al., *Fluid Ph. Equilibr.*, 2013, **352**, 100-109.